

On-Surface Synthesis of Oligo(indenoindene)

Marco Di Giovannantonio,* Qiang Chen, José I. Urgel, Pascal Ruffieux, Carlo A. Pignedoli, Klaus Müllen,* Akimitsu Narita,* and Roman Fasel*



Cite This: *J. Am. Chem. Soc.* 2020, 142, 12925–12929



Read Online

ACCESS |

Metrics & More

Article Recommendations

Supporting Information

ABSTRACT: Fully conjugated ladder polymers (CLP) possess unique optical and electronic properties and are considered promising materials for applications in (opto)electronic devices. Poly(indenoindene) is a CLP consisting of an alternating array of five- and six-membered rings, which has remained elusive so far. Here, we report an on-surface synthesis of oligo(indenoindene) on Au(111). Its structure and a low electronic band gap have been elucidated by low-temperature scanning tunneling microscopy and spectroscopy and noncontact atomic force microscopy, complemented by density functional theory calculations. Achieving defect-free segments of oligo(indenoindene) offers exclusive insight into this CLP and provides the basis to further synthetic approaches.

Conjugated ladder polymers (CLPs) have attracted extensive attention for their intriguing properties distinct from the conventional conjugated polymers.^{1–5} In virtue of their fully conjugated and rigid polymer backbone, CLPs hold promise for high mobility of charge carriers,^{6,7} long exciton diffusion length,⁸ and low energy gaps.^{5,9–14} CLPs can be synthesized by either direct ladder polymerization, simultaneously forming two covalent bonds between monomer units, or “zipping” of a prepolymer decorated with proper functional groups that can form additional bonds.^{1–3,15}

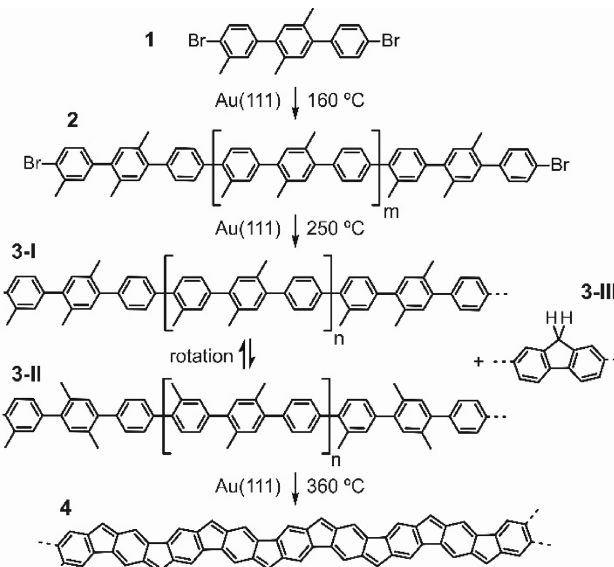
A particular class of CLPs is represented by an extension of indenofluorene¹⁶ into a polymer, that is poly(indenoindene) (PInIn), where the alternation of five- and six-membered rings gives rise to the ladder structure.^{17–20} The synthesis of PInIns was pioneered by Scherf and Müllen in 1992, but the final dehydrogenation step did not proceed completely, and unambiguous structural proof could not be obtained.²¹ More recently, Wu et al. synthesized a short segment of PInIn with four and five pentagons and hexagons, respectively,¹⁷ but more extended PInIns have remained elusive.

On-surface synthesis has become a powerful tool for the preparation of two-dimensional covalent organic frameworks and quasi-one-dimensional graphene nanoribbons with various structures and properties by rational design of small-molecule precursors.^{4,22–24} Under ultrahigh vacuum (UHV) conditions, chemical and electronic structures of the resulting products can be *in situ* visualized by scanning tunneling microscopy/spectroscopy (STM/STS) and noncontact atomic force microscopy (nc-AFM), providing their unambiguous characterizations.

Recently, we have established on-surface syntheses of indenofluorene polymers by utilizing oxidative cyclization of methyl groups against phenylene rings of polyphenylene backbones,^{25,26} an alternative strategy to dehydrogenation of dihydroindenofluorene precursors by the STM tip.²⁷ We have considered that increasing the number of methyl groups on the PPP backbone in this system can lead to PInIns. Here, we report an unprecedented on-surface synthesis of *para*-type

oligo(indenoindene) (*p*-OInIn, 4) on Au(111), starting from dibromo-trimethyl-*p*-terphenyl 1 as the precursor (Scheme 1). A sequence of thermally activated reactions led to atomically precise segments of the targeted *p*-OInIn 4, although defects, mainly due to isomerization and incomplete dehydrogenation of methylene carbons, were overall present. *p*-OInIn 4 was characterized by means of low-temperature STM/STS and nc-

Scheme 1. Reaction Pathway from 1 to *p*-OInIn 4 on Au(111)



Received: May 29, 2020

Published: July 14, 2020



AFM, complemented by density functional theory (DFT) calculations, providing structural and electronic insights into this elusive CLP.

To achieve the formation of the desired ladder polymer, precursor **1** was sublimed onto a clean Au(111) surface held at room temperature (RT) in UHV. STM images of the resulting adsorbate layer show intact molecules of precursor **1** that form self-assembled domains, stabilized by Br···H interactions (Figure 1a,b; see also Figure S1 for large scale STM images

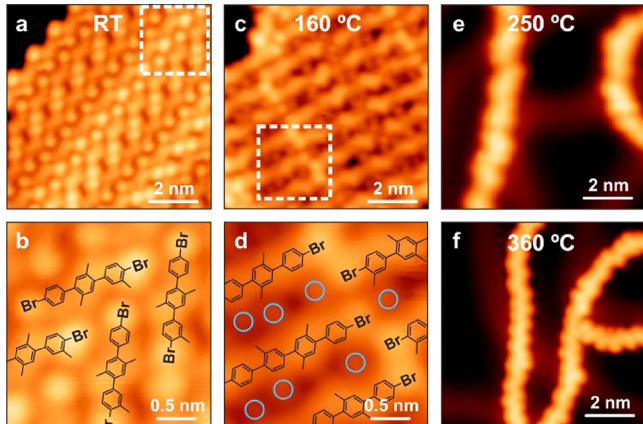


Figure 1. STM images of the Au(111) surface after deposition of precursor **1** at RT followed by repeated annealing steps at the given temperatures (a–f). (b,d) Magnified STM images of panels (a) and (c), respectively, at the positions indicated by the dashed squares, with superimposed molecular schemes. The blue circles in (d) indicate bromine atoms. Scanning parameters: (a,b) $I_t = 100 \text{ pA}$, $V_b = -0.5 \text{ V}$; (c,d) $I_t = 50 \text{ pA}$, $V_b = -0.5 \text{ V}$; (e) $I_t = 100 \text{ pA}$, $V_b = -0.5 \text{ V}$; (f) $I_t = 30 \text{ pA}$, $V_b = -0.5 \text{ V}$.

of all the investigated phases). Annealing this sample to 160 °C led to homolytic cleavage of (most of) the C–Br bonds and C–C bond formation between the generated diradical species to form methyl substituted oligo-*p*-phenylene **2**, which was still terminated with bromine atoms (Figure 1c,d).^{23,28–31} The dissociated bromine atoms chemisorbed onto the Au(111) surface and stabilized islands of packed oligomers **2**. The presence of diagonal features in the oligomer backbones suggested that the methyl groups had not reacted at this annealing step, as previously reported for similar systems.^{25,26} Oligomer **2** had a length distribution mostly ranging from 2 to 10 repeat units ($m = 0–8$ in Scheme 1). Annealing the sample to 250 °C promoted complete debromination of the terminal sites accompanied by further polymer growth. The appearance of the chains was more disordered (Figure 1e), which suggested that beyond the formation of methyl substituted poly-*p*-phenylene (PPP) chains **3**, additional reactions involving part of the methyl groups took place. Phenylene rings in polymer **3** could undergo torsional rotation, changing the alternation of methyl groups along the polymer chains (e.g., 3-I and 3-II in Scheme 1) in a dynamic manner (vide infra).²⁵ Methyl cyclization and partial dehydrogenation were initiated at this temperature, affording methylene bridges (3-III in Scheme 1) randomly distributed along the chains. The observed polymers were no longer packed into islands. This change can be attributed to the desorption of bromine atoms from the Au(111) surface, which is known to be promoted by the presence of atomic hydrogen,^{32,33} and to occur in this temperature range.³⁴ Moreover, some T-shape connections

between the polymers appeared (see Figure S1c), most likely arising from undesired coupling reactions between the terminal radicals and methyl groups on the backbones.

The oxidative cyclization of methyl groups was (nearly) completed after annealing the sample to 360 °C (Figure 1f). This on-surface reaction is most probably initiated by the homolytic cleavage of the benzylic C–H bond, namely of the methyl group, considering its higher reactivity compared to that of the phenyl C–H bond. A zigzag appearance of the resulting polymers suggested the formation of five-membered rings on alternating sides of the polymer backbones, even though long-range order of such pattern was lacking. Nevertheless, some polymer segments had a well-defined, regular spacing between the characteristic features corresponding to the five-membered rings, as visible in the STM image in Figure 2a. We subsequently performed constant-height STM

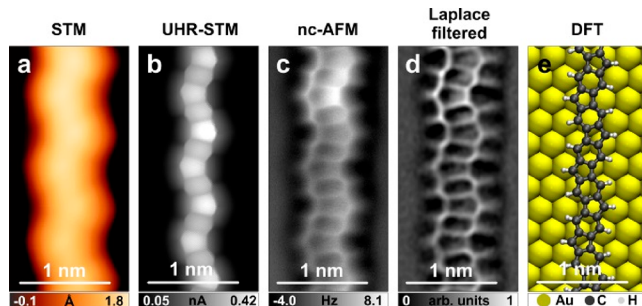


Figure 2. Images of a ladder oligomer *p*-OInIn **4** segment obtained after annealing **1** on Au(111) at 360 °C, acquired in different modes. (a) Constant-current STM image. (b) Constant-height STM image recorded with a CO-functionalized tip. (c) Constant-height frequency-shift nc-AFM image performed with a CO-functionalized tip. (d) Laplace-filtered image of (c). (e) DFT-optimized geometry of an oligomer **4** on Au(111). Scanning parameters: (a) $I_t = 50 \text{ pA}$, $V_b = -0.2 \text{ V}$; (b) Δz is 1.0 Å above the STM set point: $I_t = 100 \text{ pA}$, $V_b = -5 \text{ mV}$; (c) Δz is 2.6 Å above the STM set point: $I_t = 150 \text{ pA}$, $V_b = -5 \text{ mV}$.

imaging with a CO-functionalized tip, which resulted in the ultrahigh resolution STM (UHR-STM) image in Figure 2b. Thereby, an alternation of five- and six-membered rings could be clearly discerned. To unambiguously resolve the structure of such segments, constant-height frequency-shift nc-AFM imaging with a CO-functionalized tip³⁵ was carried out (Figure 2c). The resulting image identified the chemical structure of this segment as the desired ladder oligomer *p*-OInIn **4**. Hence, the methyl groups had cyclized to the neighboring phenylene rings, releasing two hydrogen atoms and forming methine bridges on alternating sides of the PPP backbone (Figure 2c and d).

We attribute the lack of long-range order in the position of the five-membered rings along the polymer axis to rotation of polymer subunits before cyclization (see structures 3-I and 3-II in Scheme 1). The rotation of an *ortho*-methyl substituted phenylene ring of a PPP chain on Au(111) exhibits an energy barrier of only 0.7 eV (computed by the nudged elastic band method), which can be overcome at the experimental conditions during the annealing procedure,²⁵ thus producing the observed defects. Therefore, the targeted *p*-OInIn **4** with regularly alternating five- and six-membered rings was achieved only when the methyl groups were organized with the desired consecutive alternation. In other cases, constitutional isomers of **4** with different orientations of five- and six-membered rings

were observed (see Figures 3 and S2). Figure 3 shows some examples of defective structures identified by nc-AFM.

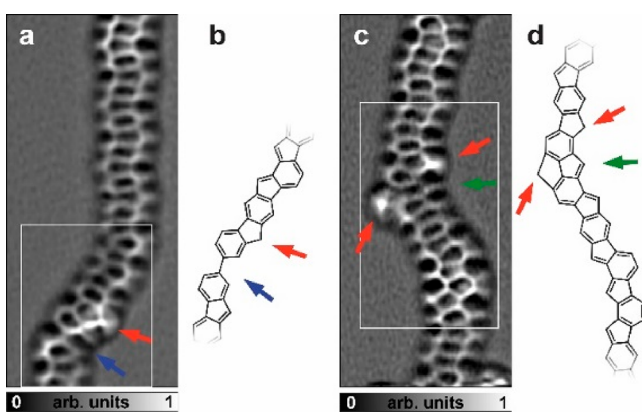


Figure 3. Laplace-filtered nc-AFM images of defective segments (see Figure S2 for the raw data) obtained after annealing **1** on Au(111) at 360 °C.

Methylene ($-\text{CH}_2-$) bridges were observed as brighter features (red arrows), which are attributed to incomplete dehydrogenation after heating at 360 °C for 10 min. The presence of two five-membered rings at the same polymer site (green arrows) was also detected, indicating that the undesired head-to-head coupling may proceed even with two *ortho*-methyl groups facing each other. Single bonds were additionally discerned (blue arrows), hindering complete ladderization. The absence of the five-membered rings at these positions may be ascribed to either (i) tail-to-tail linkage of the precursor molecules or (ii) loss of methyl groups during the annealing, as observed also in other segments (see Figure S2). From the nc-AFM images (Figures 2, 3, and S2), we could find a significant amount of defect-free units in the ladders. Regrettably, the presence of the above-mentioned irregularities (even if in small amount) limits the defect-free ladders to rather short segments of about 3 nm; hence, we identify them as oligomers *p*-OInIn **4**. However, in the following we will show that even these short segments are long enough to be representative of the electronic properties of longer ladder polymers.

After a critical assessment of the possible defects, we characterized the electronic properties of a *p*-OInIn **4**. A voltage-dependent differential conductance spectrum (dI/dV vs V) acquired on an ~3 nm long defect-free segment of **4** revealed peaks in the density of states (DOS) at -0.75 , -0.35 , and $+0.45$ V (Figure 4a). Spatial dI/dV mapping at these voltages agreed well with DFT-computed local DOS (LDOS) maps for HOMO-1, HOMO, and LUMO, respectively, for an oligomer of **4** (finite system with the length of 8.6 nm, Figure S3) adsorbed on Au(111), which confirmed the origin of the observed DOS peaks (Figures 4b–g and S4). We computed an oligomer longer than the experimentally characterized segment in order to avoid limitations due to finite-size effects (see Figure S3). The good match observed in Figure 4 shows that the experimentally investigated segment is representative of longer polymers. The band gap of *p*-OInIn **4** on Au(111) was determined to be 0.8 eV based on the dI/dV spectrum. On the other hand, DFT calculations indicated the HOMO-LUMO gap of the oligomer of **4** on Au(111) to be 0.22 eV (identified as the energy difference between HOMO and LUMO peaks of the finite oligomer in Figure S4), in accordance with the band gap value of 0.2 eV calculated for an infinite polymer **4** in the

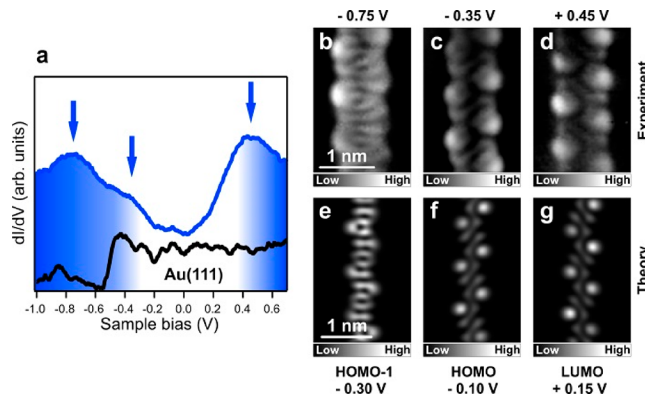


Figure 4. (a) dI/dV spectrum acquired on a segment of the ladder oligomer *p*-OInIn **4** (blue curve), and a reference spectrum taken on the bare Au(111) surface (black curve). Three main signals arise from **4** at -0.75 , -0.35 , and 0.45 V. (b–d) Constant-current dI/dV maps at the indicated voltages, corresponding to the main features observed in (a). (e–g) Theoretical dI/dV maps of HOMO-1, HOMO, and LUMO of an oligomer **4** adsorbed on Au(111) (the full maps are shown in Figure S3).

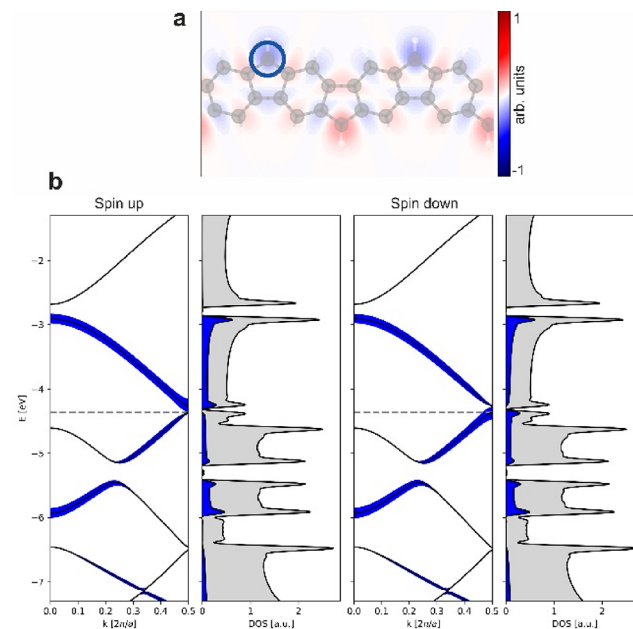


Figure 5. (a) Spin density map of polymer **4** in gas phase. (b) Band structure and DOS. The blue lines in the band structure and the filled blue DOS indicate the corresponding bands/DOS, respectively, to originate from states that have major contributions from the carbon atom at the apex of the five-membered rings (blue circle in panel a).

gas phase (Figure 5). These theoretical energy gaps are in line with the experimental observations, considering the typical underestimation of DFT computed band gaps.³⁶ Furthermore, DFT gas phase calculations for the infinite polymer revealed that **4** is spin-polarized with spin density antiferromagnetically located at the five-membered ring apices (Figure 5a). Additionally, we found that the methine carbons at the five-membered ring apices contribute to the lower conduction band and the second half of the upper valence band (Figure 5), highlighting the role of these nonbenzenoid rings in the electronic structure of **4**. A complete assignment of the other bands is reported in Figure S5.

In conclusion, we have demonstrated the on-surface synthesis of oligo(indenoindene) **4** via sequential aryl–aryl coupling of *p*-terphenyl-based precursor **1** and cyclization of methyl substituents. Although formation of constitutional isomers and incomplete dehydrogenation were observed, defect-free segments of **4** could be clearly visualized by nc-AFM. Detailed electronic characterizations by STS and DFT calculations revealed a low band gap and the antiferromagnetic character of **4**. Alternative monomer designs are currently considered in our laboratories to achieve such conjugated ladder polymers with high regioselectivity, for electronic device applications and experimental elucidation of their magnetic properties.

■ ASSOCIATED CONTENT

Supporting Information

The Supporting Information is available free of charge at <https://pubs.acs.org/doi/10.1021/jacs.0c05701>.

Crystallographic data for **1** ([CIF](#))

Synthesis of the molecular precursor **1**; experimental and theoretical methods; additional experimental and theoretical results ([PDF](#))

■ AUTHOR INFORMATION

Corresponding Authors

Marco Di Giovannantonio — *Empa, Swiss Federal Laboratories for Materials Science and Technology, nanotech@surfaces Laboratory, 8600 Dübendorf, Switzerland;*  orcid.org/0000-0001-8658-9183; Email: marco.digiovannantonio@empa.ch

Klaus Müllen — *Max Planck Institute for Polymer Research, 55128 Mainz, Germany; Institute of Physical Chemistry, Johannes Gutenberg University Mainz, 55128 Mainz, Germany;*  orcid.org/0000-0001-6630-8786; Email: muellen@mpip-mainz.mpg.de

Akimitsu Narita — *Max Planck Institute for Polymer Research, 55128 Mainz, Germany; Organic and Carbon Nanomaterials Unit, Okinawa Institute of Science and Technology Graduate University, Okinawa 904-0495, Japan;*  orcid.org/0000-0002-3625-522X; Email: narita@mpip-mainz.mpg.de

Roman Fasel — *Empa, Swiss Federal Laboratories for Materials Science and Technology, nanotech@surfaces Laboratory, 8600 Dübendorf, Switzerland; Department of Chemistry and Biochemistry, University of Bern, 3012 Bern, Switzerland;*  orcid.org/0000-0002-1553-6487; Email: roman.fasel@empa.ch

Authors

Qiang Chen — *Max Planck Institute for Polymer Research, 55128 Mainz, Germany;*  orcid.org/0000-0001-5612-1504

José I. Urgel — *Empa, Swiss Federal Laboratories for Materials Science and Technology, nanotech@surfaces Laboratory, 8600 Dübendorf, Switzerland;*  orcid.org/0000-0001-7608-2979

Pascal Ruffieux — *Empa, Swiss Federal Laboratories for Materials Science and Technology, nanotech@surfaces Laboratory, 8600 Dübendorf, Switzerland;*  orcid.org/0000-0001-5729-5354

Carlo A. Pignedoli — *Empa, Swiss Federal Laboratories for Materials Science and Technology, nanotech@surfaces Laboratory, 8600 Dübendorf, Switzerland;*  orcid.org/0000-0002-8273-6390

Complete contact information is available at:

<https://pubs.acs.org/10.1021/jacs.0c05701>

Notes

The authors declare no competing financial interest.

■ ACKNOWLEDGMENTS

This work was supported by the Swiss National Science Foundation under Grant No. 200020_182015, the NCCR MARVEL funded by the Swiss National Science Foundation (S1NF40-182892), the European Union's Horizon 2020 research and innovation program under Grant Agreement Number 785219 (Graphene Flagship Core 2), the Max Planck Society, and the Office of Naval Research (N00014-18-1-2708). Computational support from the Swiss Supercomputing Center (CSCS) under Project ID s904 is gratefully acknowledged. We are thankful to Lukas Rotach (Empa) for his excellent technical support during the experiments and to Dr. Dieter Schollmeyer (Johannes Gutenberg-Universität Mainz) for single crystal X-ray diffraction analysis.

■ REFERENCES

- (1) Zhu, C.; Kalin, A. J.; Fang, L. Covalent and Noncovalent Approaches to Rigid Coplanar π -Conjugated Molecules and Macromolecules. *Acc. Chem. Res.* **2019**, *52* (4), 1089–1100.
- (2) Cai, Z.; Awais, M. A.; Zhang, N.; Yu, L. Exploration of Syntheses and Functions of Higher Ladder-Type π -Conjugated Heterocenes. *Chem.* **2018**, *4* (11), 2538–2570.
- (3) Lee, J.; Kalin, A. J.; Yuan, T.; Al-Hashimi, M.; Fang, L. Fully Conjugated Ladder Polymers. *Chem. Sci.* **2017**, *8* (4), 2503–2521.
- (4) Sakamoto, J.; van Heijst, J.; Lukin, O.; Schlüter, A. D. Two-Dimensional Polymers: Just a Dream of Synthetic Chemists? *Angew. Chem., Int. Ed.* **2009**, *48* (6), 1030–1069.
- (5) Scherf, U. Ladder-Type Materials. *J. Mater. Chem.* **1999**, *9* (9), 1853–1864.
- (6) Prins, P.; Grozema, F. C.; Schins, J. M.; Patil, S.; Scherf, U.; Siebbeles, L. D. A. High Intrachain Hole Mobility on Molecular Wires of Ladder-Type Poly(p-Phenylens). *Phys. Rev. Lett.* **2006**, *96* (14), 146601.
- (7) Babel, A.; Jenekhe, S. A. High Electron Mobility in Ladder Polymer Field-Effect Transistors. *J. Am. Chem. Soc.* **2003**, *125* (45), 13656–13657.
- (8) Samiullah, M.; Moghe, D.; Scherf, U.; Guha, S. Diffusion Length of Triplet Excitons in Organic Semiconductors. *Phys. Rev. B: Condens. Matter Mater. Phys.* **2010**, *82* (20), 205211.
- (9) Tsuda, A.; Osuka, A. Fully Conjugated Porphyrin Tapes with Electronic Absorption Bands That Reach into Infrared. *Science* **2001**, *293* (5527), 79–82.
- (10) Yang, W.; Lucotti, A.; Tommasini, M.; Chalifoux, W. A. Bottom-Up Synthesis of Soluble and Narrow Graphene Nanoribbons Using Alkyne Benzannulations. *J. Am. Chem. Soc.* **2016**, *138* (29), 9137–9144.
- (11) Wu, Y.; Zhang, J.; Fei, Z.; Bo, Z. Spiro-Bridged Ladder-Type Poly(p-Phenylene)s: Towards Structurally Perfect Light-Emitting Materials. *J. Am. Chem. Soc.* **2008**, *130* (23), 7192–7193.
- (12) Piok, T.; Gamerith, S.; Gadermaier, C.; Plank, H.; Wenzl, F. P.; Patil, S.; Montenegro, R.; Kietzke, T.; Neher, D.; Scherf, U.; Landfester, K.; List, E. J. W. Organic Light-Emitting Devices Fabricated from Semiconducting Nanospheres. *Adv. Mater.* **2003**, *15* (10), 800–804.
- (13) Durban, M. M.; Kazarinoff, P. D.; Segawa, Y.; Luscombe, C. K. Synthesis and Characterization of Solution-Processable Laddered n-Type Naphthalene Bisimide Copolymers for OFET Applications. *Macromolecules* **2011**, *44* (12), 4721–4728.
- (14) Babel, A.; Jenekhe, S. A. Electron Transport in Thin-Film Transistors from an n-Type Conjugated Polymer. *Adv. Mater.* **2002**, *14* (5), 371–374.

- (15) Yano, Y.; Mitoma, N.; Matsushima, K.; Wang, F.; Matsui, K.; Takakura, A.; Miyauchi, Y.; Ito, H.; Itami, K. Living Annulative π -Extension Polymerization for Graphene Nanoribbon Synthesis. *Nature* **2019**, *571* (7765), 387–392.
- (16) Tobe, Y. Non-Alternant Non-Benzenoid Aromatic Compounds: Past, Present, and Future. *Chem. Rec.* **2015**, *15* (1), 86–96.
- (17) Hu, P.; Lee, S.; Herng, T. S.; Aratani, N.; Gonçalves, T. P.; Qi, Q.; Shi, X.; Yamada, H.; Huang, K.-W.; Ding, J.; Kim, D.; Wu, J. Toward Tetraradicaloid: The Effect of Fusion Mode on Radical Character and Chemical Reactivity. *J. Am. Chem. Soc.* **2016**, *138* (3), 1065–1077.
- (18) Kertesz, M. Structure and Electronic Structure of Low-Band-Gap Ladder Polymers. *Macromolecules* **1995**, *28* (5), 1475–1480.
- (19) Fukuda, K.; Fujiyoshi, J.; Matsui, H.; Nagami, T.; Takamuku, S.; Kitagawa, Y.; Champagne, B.; Nakano, M. A Theoretical Study on Quasi-One-Dimensional Open-Shell Singlet Ladder Oligomers: Multi-Radical Nature, Aromaticity and Second Hyperpolarizability. *Org. Chem. Front.* **2017**, *4* (5), 779–789.
- (20) Yamane, M.; Kishi, R.; Tonami, T.; Okada, K.; Nagami, T.; Kitagawa, Y.; Nakano, M. Open-Shell Characters, Aromaticities and Third-Order Nonlinear Optical Properties of Carbon Nanobelts Composed of Five- and Six-Membered Rings. *Asian J. Org. Chem.* **2018**, *7* (11), 2320–2329.
- (21) Scherf, U.; Müllen, K. Polyarylenes and Poly(Arylenevinylene)-s: 8. The First Soluble Ladder Polymer with 1,4-Benzoquinone-Bismethide Subunits. *Polymer* **1992**, *33* (11), 2443–2446.
- (22) Talirz, L.; Ruffieux, P.; Fasel, R. On-Surface Synthesis of Atomically Precise Graphene Nanoribbons. *Adv. Mater.* **2016**, *28* (29), 6222–6231.
- (23) Di Giovannantonio, M.; Contini, G. Reversibility and Intermediate Steps as Key Tools for the Growth of Extended Ordered Polymers via On-Surface Synthesis. *J. Phys.: Condens. Matter* **2018**, *30*, 093001.
- (24) Lindner, R.; Kühnle, A. On-Surface Reactions. *ChemPhysChem* **2015**, *16* (8), 1582–1592.
- (25) Di Giovannantonio, M.; Urgel, J. I.; Beser, U.; Yakutovich, A. V.; Wilhelm, J.; Pignedoli, C. A.; Ruffieux, P.; Narita, A.; Müllen, K.; Fasel, R. On-Surface Synthesis of Indenofluorene Polymers by Oxidative Five-Membered Ring Formation. *J. Am. Chem. Soc.* **2018**, *140* (10), 3532–3536.
- (26) Di Giovannantonio, M.; Eimre, K.; Yakutovich, A. V.; Chen, Q.; Mishra, S.; Urgel, J. I.; Pignedoli, C. A.; Ruffieux, P.; Müllen, K.; Narita, A.; Fasel, R. On-Surface Synthesis of Antiaromatic and Open-Shell Indeno[2,1-b]Fluorene Polymers and Their Lateral Fusion into Porous Ribbons. *J. Am. Chem. Soc.* **2019**, *141* (31), 12346–12354.
- (27) Majzik, Z.; Pavliček, N.; Vilas-Varela, M.; Pérez, D.; Moll, N.; Gutián, E.; Meyer, G.; Peña, D.; Gross, L. Studying an Antiaromatic Polycyclic Hydrocarbon Adsorbed on Different Surfaces. *Nat. Commun.* **2018**, *9* (1), 1198.
- (28) Grill, L.; Dyer, M.; Lafferentz, L.; Persson, M.; Peters, M. V.; Hecht, S. Nano-Architectures by Covalent Assembly of Molecular Building Blocks. *Nat. Nanotechnol.* **2007**, *2* (11), 687–691.
- (29) Di Giovannantonio, M.; El Garah, M.; Lipton-Duffin, J.; Meunier, V.; Cardenas, L.; Fagot Revurat, Y.; Cossaro, A.; Verdini, A.; Perepichka, D. F.; Rosei, F.; Contini, G. Insight into Organometallic Intermediate and Its Evolution to Covalent Bonding in Surface-Confined Ullmann Polymerization. *ACS Nano* **2013**, *7* (9), 8190–8198.
- (30) Di Giovannantonio, M.; El Garah, M.; Lipton-Duffin, J.; Meunier, V.; Cardenas, L.; Fagot-Revurat, Y.; Cossaro, A.; Verdini, A.; Perepichka, D. F.; Rosei, F.; Contini, G. Reply to “Comment on ‘Insight into Organometallic Intermediate and Its Evolution to Covalent Bonding in Surface-Confined Ullmann Polymerization’”. *ACS Nano* **2014**, *8* (3), 1969–1971.
- (31) Cai, J.; Ruffieux, P.; Jaafar, R.; Bieri, M.; Braun, T.; Blankenburg, S.; Muoth, M.; Seitsonen, A. P.; Saleh, M.; Feng, X.; Müllen, K.; Fasel, R. Atomically Precise Bottom-up Fabrication of Graphene Nanoribbons. *Nature* **2010**, *466* (7305), 470–473.
- (32) Bronner, C.; Björk, J.; Tegeder, P. Tracking and Removing Br during the On-Surface Synthesis of a Graphene Nanoribbon. *J. Phys. Chem. C* **2015**, *119* (1), 486–493.
- (33) Mairena, A.; Baljozovic, M.; Kawecki, M.; Grenader, K.; Wienke, M.; Martin, K.; Bernard, L.; Avarvari, N.; Terfort, A.; Ernst, K.-H.; Wackerlin, C. The Fate of Bromine after Temperature-Induced Dehydrogenation of on-Surface Synthesized Bisheptahelicene. *Chem. Sci.* **2019**, *10* (10), 2998–3004.
- (34) Di Giovannantonio, M.; Deniz, O.; Urgel, J. I.; Widmer, R.; Dienel, T.; Stoltz, S.; Sánchez-Sánchez, C.; Muntwiler, M.; Dumslaff, T.; Berger, R.; Narita, A.; Feng, X.; Müllen, K.; Ruffieux, P.; Fasel, R. On-Surface Growth Dynamics of Graphene Nanoribbons: The Role of Halogen Functionalization. *ACS Nano* **2018**, *12* (1), 74–81.
- (35) Gross, L.; Mohn, F.; Moll, N.; Liljeroth, P.; Meyer, G. The Chemical Structure of a Molecule Resolved by Atomic Force Microscopy. *Science* **2009**, *325* (5944), 1110–1114.
- (36) Perdew, J. P. Density Functional Theory and the Band Gap Problem. *Int. J. Quantum Chem.* **1985**, *28* (S19), 497–523.